sustainability

MDPI

Article

Land Use Pattern Changes and the Driving Forces in the Shiyang River Basin from 2000 to 2018

Juan Li [1,2,3], Xunzhou Chunyu [4,*] and Feng Huang [4]

[1] Hunan Polytechnic of Water Resources and Electric Power, Changsha 410114, China
[2] School of Hydraulic and Environmental Engineering, Changsha University of Science & Technology, Changsha 410114, China
[3] Key Laboratory of Dongting Lake Aquatic Eco-Environmental Control and Restoration of Hunan Province, Changsha 410114, China
[4] College of Hydrology and Water Resources, Hohai University, Nanjing 210098, China
* Correspondence: zodiacnix@163.com

Abstract: Thorough understanding of the evolution processes and drivers behind the formation of and changes in land use and land cover (LULC) is essential for maintaining the balance between humans and fragile nature in arid regions. This quantitative driving analysis provides in-depth insight into the driving mechanisms behind the formation of and changes in LULC through a case study of the Shiyang River Basin in Northwest China. Based on land use, meteorological, topographic, and socioeconomic data from 2000 to 2018 (2000, 2005, 2010, 2015, and 2018), this study employed land use transfer matrices and the GeoDetector model to explore the evolution and driving forces behind the formation of and variations in the LULC patterns. The results demonstrated that anthropic factors mainly drove the spatial distributions of cropland and settlement. The spatial distributions of the forest, grassland, and bare land were determined by the mutual influence of natural and anthropic factors. The LULC patterns exhibited consequential variations throughout the study period. Through the occupation of the surrounding cropland and grassland, urbanization expanded rapidly. The ecological environment had been improved, but there were still considerable areas of degraded land, characterized by the grassland degradation downstream and the forest degradation upstream. Geographical differentiation was the primary driver for the transformation of bare land to grassland. The main driving forces behind urban expansion and forest loss were socioeconomic development and geographical differentiation. The degree of a certain LULC change varied among different levels of its driving factor. This research can provide scientific advice for administrators and policymakers to formulate scientific, rational, and targeted land use planning and policies in the future to achieve the sustainable development of endorheic river basins.

Keywords: land use and land cover; spatiotemporal pattern; driving forces; GeoDetector; arid endorheic river basin

Citation: Li, J.; Chunyu, X.; Huang, F. Land Use Pattern Changes and the Driving Forces in the Shiyang River Basin from 2000 to 2018. *Sustainability* **2023**, *15*, 154. https://doi.org/10.3390/su15010154

Academic Editor: Longshan Zhao

Received: 6 November 2022
Revised: 12 December 2022
Accepted: 20 December 2022
Published: 22 December 2022

1. Introduction

Endorheic river basins, mainly distributed in arid and semiarid areas, account for 11.4% of the global land area [1]. Owing to the extreme scarcity of water resources and relatively simple ecosystems, the environment of endorheic river basins is attributed to high ecological sensitivity and vulnerability [2]. In the past few decades, with rapid population growth and socioeconomic development, natural resources in endorheic river basins have been exploited and utilized extensively, resulting in tremendous LULC changes [3]. As the interface between natural and human systems and representing a significant challenge for sustainable development, LULC changes contribute prominently to ecological degradation, including, but not limited to, land desertification, biodiversity loss,

vegetation coverage declines, and terminal lake shrinkage in many endorheic river basins [4,5], such as the Aral Sea [6], Tarim River [7], Heihe River [8], etc.

As a result of complicated human–environment interactions, LULC and its changes are generally recognized as being driven by both anthropic and natural factors. The great codependencies in the socioecological systems make it hard to ascertain the primary causes [9]. Nonetheless, investigating the evolution processes of LULC and identifying the predominant drivers of LULC formation and its changes are critical for sustaining the equilibrium between human and fragile nature, as well as for arranging practical strategies for land use planning and environmental conservation [5,10]. Therefore, research on LULC is urgent and crucial for conserving the fragile environment and realizing sustainable development in arid endorheic river basins, which has attracted attention from scholars worldwide. To the best of our knowledge, prior research on LULC in arid endorheic river basins have mainly focused on four aspects: (1) analysis of LULC evolution and its driving forces [9,11–14]; (2) analysis of landscape pattern characteristics evolution [15–18]; (3) simulations and prediction analysis of LULC change [19–21]; and (4) assessing the ecological and hydrological effects caused by LULC change [8,22–24]. Additionally, most of the previous studies of the driving forces behind LULC mainly focused on qualitative descriptions [11,12,24,25]. Only a few studies have involved quantitatively analyzing the driving forces behind LULC pattern formation and LULC changes in endorheic river basins [4,26]. However, most prior quantitative analyses used techniques such as principal component analysis [17,26] and analytic hierarchy process [27]. These methods initially have some fuzziness, and cannot clearly and quantitatively determine the effects of individual driving factors of LULC. Secondly, when dividing the weight of various factors, the subjectivity is too strong to objectively ascertain the optimal weight ratio [28,29]. Knowledge gaps exist in quantitatively exploring the drivers of LULC formation and its change in endorheic river basins. Additionally, further knowledge of how the driving forces affect LULC is required. Effective and quantitative investigations of the driving factors and mechanisms of LULC formation and variation are indispensable for providing scientific references for ecological protection and LULC optimization in arid endorheic basins.

This study applied land use transfer matrices, a GeoDetector, and remote sensing technology to fill the preceding knowledge gaps through a systematic and quantitative investigation into the spatiotemporal evolution and driving forces behind the formation of and changes in LULC in the Shiyang River Basin (SRB). The SRB is a representative endorheic river basin in the arid region of Northwest China that has undergone severe degradation of vegetation, significant reduction in groundwater, and the aggravation of desertification due to intense socioeconomic development over the past few decades [30]. Land use transfer matrices and GeoDetector have been widely used in LULC evolution and driving analyses [31,32]. Land use transfer matrices and remote sensing techniques were adopted to investigate the spatiotemporal characteristics of LULC and its variations in the endorheic river basin. Compared with regression analysis, the GeoDetector model is more efficient and convenient due to its immunity to collinearity among factors [33]. Therefore, GeoDetector was adopted to quantitatively identify the driving factors of LULC formation and its change in the endorheic river basin. This study aimed to: (1) quantitatively analyze the composition, structure, and spatial distribution patterns of LULC; (2) identify the spatiotemporal evolution characteristics of LULC patterns and the main LULC change types from 2000 to 2018; (3) quantitatively detect the driving forces behind the formation of LULC patterns in different periods and the driving forces behind the main LULC change types in the SRB. This study can enrich the comprehension of the mechanisms of LULC formation and variations in the arid endorheic river basin and afford scientific evidence for land use policymakers and administrators to formulate more scientific and rational land use strategies. Furthermore, the study area is representative of the expansive arid landscapes in Northwest China, which can provide a reference for LULC research in other comparable arid endorheic river basins.

2. Study Area

The Shiyang River originates in the southeastern part of the Qilian Mountains in Northwest China, flows through the cities of Wuwei and Jinchang, and finally disappears into the Minqin Oasis between the Tengger Desert and the Badain Jaran Desert (Figure 1). The entire basin is located in the central part of Gansu Province, which lies in the easternmost part of the Hexi Corridor (101°41′–104°16′ E, 36°29′–39°27′ N) [34]. The study area covers 39,492 km², and the elevation ranges from 1222 to 4834 m. It is generally characterized by a continental temperate arid and semiarid climate, with intense solar radiation, sufficient sunshine, significant temperature difference, little precipitation, and intense evaporation [35].

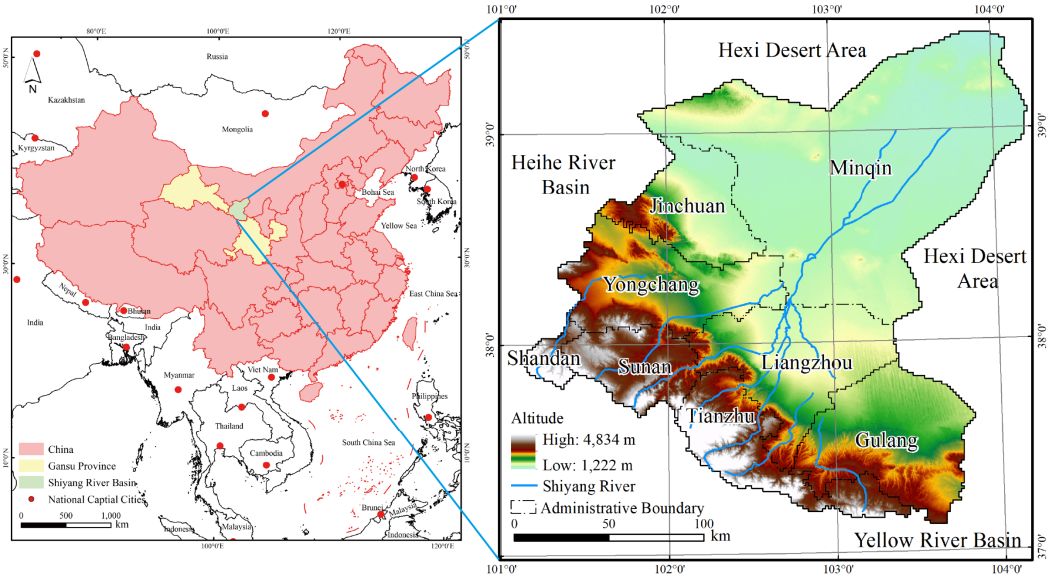

Figure 1. Geographical location of the SRB.

Due to the arid climate, the limited water resources make the whole basin's ecological environment extremely fragile. With the development of high-intensity anthropogenic activities over more than half a century, especially the rapid development and expansion of industry and agriculture in the densely populated middle and lower reaches of the SRB since the implementation of the Western Development Strategy by the Chinese government, water and soil resources have been utilized on a large scale. Therefore, increasing water demand and excessively irrational exploitation have resulted in a sharp contradiction between industrial, agricultural, and ecological water across the entire basin [36]. A large amount of ecological water has been occupied, leading to large-scale vegetation degradation, desertification, and other serious ecological and environmental problems in the SRB. With the implementation of several ecological environment protection policies, such as the Grain for Green Project and the Key Treatment Program of the Shiyang River Basin, proposed in 1999 and 2007, respectively, many unreasonable land exploitation proposals have been restricted and controlled. The ecological environment has been improved to some degree in many areas of the SRB [13].

3. Data and Methods

The flowchart can be practically divided into three sections (Figure 2). The first section was to collect datasets for analysis in this research. Next was to investigate the composition structure, evolution trend features of the LULC pattern, and the main LULC change types in the SRB. Finally, the driving factors behind the formation and evolution of the LULC patterns in the SRB were investigated.

The land use dataset of the SRB from 2000 to 2018 was selected to analyze the LULC structure and spatial distribution. The land use transfer matrix was employed to explore the temporal evolution features of the main LULC categories, and the major LULC changes in the SRB from 2000 to 2018 were obtained. Eleven indicators involving the climate, topography, and human activities were chosen as potential driving factors. The spatial patterns of each potential factor in different time periods and variations of each factor throughout the study period were collected as independent variables for the recognition of different driving forces. Driving analyses of land use patterns at different times nodes and the main LULC change types during the whole study period in the SRB were conducted through GeoDetector. Finally, the implications were discussed for LULC planning in the SRB to achieve the sustainable development of the SRB. The specific analysis data and methods are demonstrated in Figure 2.

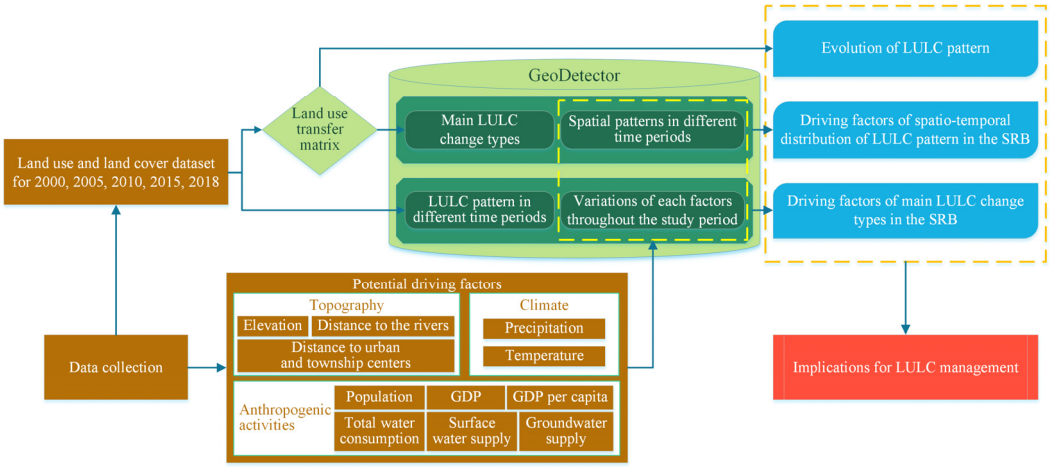

Figure 2. The framework for the analysis of land use pattern changes and the driving forces.

3.1. Data Collection and Processing

The data used were composed of four main categories: land use, topographic, meteorological, and socioeconomic data of the SRB from 2000 to 2018. Owing to the long, relatively high-resolution time-series and good classification accuracy in China [37–40], land use data from the Climate Change Initiative-Land Cover (CCI-LC) provided by the European Space Agency (ESA) with a spatial resolution of 300 m (http://www.esa-landcover-cci.org/ (accessed on 1 March 2020)) were chosen. The raw CCI-LC data have divided the LULC types into 22 categories. According to relevant research [37,41,42], and considering the features of the SRB, the land use data were reclassified into six classification types: cropland, forest, grassland, settlement, bare land, and others. The ASTER GDEM V3 (Advanced Spaceborne Thermal Emission and Reflection Radiometer Global Digital Elevation Model Version 3) series datasets provided by NASA with a 30 m resolution were used for DEM data. These were mainly used in two aspects: (1) as a potential influencing factor representing the topography of the basin to analyze the driving forces behind the LULC spatial patterns and LULC change in the SRB; and (2) a covariable in the spatial interpolation of climatic data. The data of the river system, urban areas, and township centers of the SRB were downloaded from the National Geomatics Center of China (http://www.ngcc.cn/ngcc/ (accessed on 1 March 2020)). Based on the original data, the Euclidean distance calculation toolbox in the ArcGIS spatial analysis module was adopted to determine the raster data of the distance to the rivers and distance to urban and township centers.

The monthly datasets of China's surface climate were collected from the China Meteorological Data Network (http://data.cma.cn (accessed on 15 March 2020)). The precipitation and temperature data of 151 weather stations within the SRB and its surrounding regions were selected based on the initial data (see Appendix A: Figure A1). The annual

mean temperature and annual accumulated precipitation of these stations selected at different time nodes (2000, 2005, 2010, 2015, and 2018) were computed. Then, spatial interpolation was performed on the annual mean temperature and annual accumulated precipitation at different study time nodes in the region. This was performed with ANUSPLIN software, which was based upon partial thin-plate smoothing spline and incorporated DEM as a covariable to help improve the interpolation accuracy. The detailed interpolation principle, method, and steps of ANUSPLIN are presented elsewhere in the relevant literature [43,44]. The grid data of the annual mean temperature and annual accumulated precipitation were used to reflect the basin's climate change for the subsequent driving-force analysis.

Population density, GDP, and GDP per capita data of the cities and counties during the period of 2000–2018 in the SRB were collected from the "*Gansu Development Yearbook*", selected as indicators representing the socioeconomic development. Meanwhile, data of the total water consumption, surface water supply, and groundwater supply were obtained from the "*Gansu Water Resources Bulletin*", which were chosen as factors reflecting the situations of water resource supply and consumption in the SRB in different years. The basin boundary data were downloaded from the Resource and Environment Science and Data Center (http://www.rescdc.cn (accessed on 1 March 2020)). Based on the primary statistical data of these six indicators, their raster data were generated using the ordinary Kriging interpolation module in ArcGIS software and were combined with the urban and township centers data.

The raster data of all the above factors were uniformly set to the WGS84 (World Geodetic System 84) Albers projected coordinate system, and the spatial resolutions were all resampled to 300 m, which were the same as the resolution of the land use data to facilitate the subsequent analysis. Finally, the raster data of each factor in the SRB were obtained through clipping according to the basin boundary.

3.2. Methods

3.2.1. Land Use Transfer Matrix

Land use transfer matrix comprehensively characterizes the mutual conversion among LULC types during a certain period in the research area. It can quantitatively indicate the transfer direction and area among various LULC types, which provides detailed "from-to" change class information [13,45]. It can be expressed as follows:

$$S_{ij}=\begin{bmatrix} S_{11} & S_{12} & \cdots & S_{1n} \\ S_{21} & S_{22} & \cdots & S_{2n} \\ \vdots & \vdots & \ddots & \vdots \\ S_{n1} & S_{n2} & \cdots & S_{nn} \end{bmatrix} \quad (1)$$

where i and j represent the LULC type at the start and the end of the study period, respectively; n is the overall number of LULC categories in the study area; and S_{ij} is the conversion area from the ith to the jth LULC type during the study period. In this research, ArcGIS 10.7 software was applied to determine the LULC changes. All land use data in distinct study times nodes were initially converted into vector data. Then, the fusion tool in ArcGIS was utilized to merge the identical land use types with each other for each land use data. The land use data for two time periods were intersected to extract the land use types in the same location from the data at different time periods. Subsequently, using Excel's pivot table function, land use transfer matrices were generated, consisting of rows and columns, which presented land use categories at the start and at the end of the study period, respectively. Based on the land use data, land use transfer matrices of the SRB in five periods were computed in this study, including 2000–2005, 2005–2010, 2010–2015, 2015–2018, and 2000–2018. Furthermore, the Mann–Kendall (MK) test was applied to assess the trends in major LULC categories during 2000–2018.

3.2.2. Attribution Analysis of LULC Spatial Distribution Patterns and LULC Changes

1. Factors Selection and Preprocessing

The SRB is a typical arid inland basin with droughts and scarce rainfall, significant spatial heterogeneity of temperature and precipitation, water resource shortages, and a prominent contradiction between rapid social and economic development and ecological protection. Hence, in this study, eleven factors related to climate change, topography, and anthropogenic activities were selected as potential influencing factors for the analysis of spatial distribution patterns and changes in LULC in the SRB. The attribution analysis in this research was mainly composed of two aspects: (1) the attribution analysis of spatial distribution patterns of LULC in different times; and (2) the attribution analysis of the main LULC change types throughout the whole study period. For the attribution analysis of LULC spatial patterns, the dependent variable was the total area of major LULC types in the SRB for different time nodes within the study period, which were counted with the zonal statistics toolbox in ArcGIS. The independent variables were the statistics of each factor corresponding to the same period. For the attribution analysis of LULC change, the dependent variable was the area of major LULC change categories in the SRB during 2000–2018. The independent variables were the variations in different factors, except for elevation, distance to the rivers, and distance to urban and township centers, using the statistics for factors in 2018 minus the statistics in 2000 to express the changes in climate and anthropogenic activities during the research period. Specific parameters are detailed in Tables 1 and 2. The GeoDetector model can only handle discrete independent variables [33]; therefore, the eleven continuous independent variables were converted into discrete variables using the reclassify tool in ArcGIS. Detailed discretization methods for each factor are described in Table A1 in Appendix B.

Table 1. Variables in the driving forces analysis of LULC patterns in the SRB.

Variable	Code	Description
Dependent variable	CLA	The area of cropland in a grid cell.
	FSA	The area of forest in a grid cell.
	GLA	The area of grassland in a grid cell.
	SLA	The area of settlement in a grid cell.
	BLA	The area of bare land in a grid cell.
Independent variable	X1	The annual mean temperature in a grid cell.
	X2	The annual accumulated precipitation in a grid cell.
	X3	The altitude in a grid cell.
	X4	The population in a grid cell.
	X5	The GDP in a grid cell.
	X6	The GDP per capita in a grid cell.
	X7	The total water consumption in grid cell.
	X8	The surface water supply in a grid cell.
	X9	The groundwater supply in a grid cell.
	X10	The distance to the rivers in a grid cell.
	X11	The distance to urban and township centers in a grid cell.

Table 2. Variables in the driving forces analysis of LULC patterns in the SRB.

Variable	Code	Description
Dependent variable	CTG	The area of conversion of cropland to grassland in a grid cell.
	CTS	The area of conversion of cropland to settlement in a grid cell.
	FTG	The area of conversion of forest to grassland in a grid cell.
	GTB	The area of conversion of grassland to bare land in a grid cell.
	GTC	The area of conversion of grassland to cropland in a grid cell.
	GTS	The area of conversion of grassland to settlement in a grid cell.
	BTC	The area of conversion of bare land to cropland in a grid cell.
	BTG	The area of conversion of bare land to grassland in a grid cell.
	OTS	The area of conversions of other land use types.
	CTG	The area of conversion of cropland to grassland in a grid cell.
Independent variable	Z1	The change in annual mean temperature in a grid cell.
	Z2	The change in annual accumulated precipitation in a grid cell.
	Z3	The altitude in a grid cell.
	Z4	The change in population in a grid cell.
	Z5	The change in GDP in a grid cell.
	Z6	The change in GDP per capita in a grid cell.
	Z7	The change in total water consumption in grid cell.
	Z8	The change in surface water supply in a grid cell.
	Z9	The change in groundwater supply in a grid cell.
	Z10	The distance to the rivers in a grid cell.
	Z11	The distance to urban and township centers in a grid cell.

2. GeoDetector model

In this research, the GeoDetector model was adopted to analyze the driving forces behind the spatial distribution patterns and changes in LULC in the SRB. It is a statistical approach to explore spatial heterogeneity and reveal the driving forces behind the spatial heterogeneity. The software was available on the website (http://geodetector.cn/ (accessed on 1 March 2020)), and in this study it was executed with the version for Excel. GeoDetector has no linear hypothesis, and its core idea is that, if an independent variable has a significant influence on a dependent variable, their spatial pattern should be similar. Moreover, the basic principle of GeoDetector is the assumption that the research region is separated into several subregions. If the sum of the variance in subregions is less than the overall variance of the region, there is spatial heterogeneity; if the spatial pattern of the two variables tends to be the same, a statistical correlation exists between them [33,46].

GeoDetector consists of four detectors: a factor detector, an interaction detector, a risk detector, and an ecological detector. The factor detector is employed to quantitatively identify the driving factors affecting the dependent variable. The q statistic measures the explanatory power of each factor, and its expression is defined as follows:

$$q = 1 - \frac{1}{N\sigma^2}\sum_{h=1}^{L} N_h \sigma_h^2 \quad (2)$$

where q represents the explanatory power of one factor on the spatial patterns of major LULC types (such as cropland), or the explanatory power of one factor on the main LULC change types (such as the conversion of cropland to settlement); $h = 1, \ldots, L$ is the strata or partitions of factor X or Z; N_h and N denote the number of grid cells of the stratum h and the whole region, respectively; σ_h^2 and σ^2 are the variances in the dependent variable in the stratum h and the whole region, respectively. The q statistic ranges from 0 to 1. The greater the value of q, the stronger the explanatory power of the factor on the dependent variable, and vice versa. If $q = 1$, it means that the factor completely dominates the spatial

pattern of the dependent variable, and $q = 0$ if the factor is entirely irrelevant to the dependent variable. The q value denotes that the factor explains $100 \times q\%$ of the dependent variable. The q statistic was fitted to the noncentral F distribution, which was applied to detect the significance level [33].

In this study, attribution analysis was mainly carried out in two aspects. One was the attribution analysis of the spatial patterns of LULC in different time nodes in the SRB. Thus, the q statistics of eleven factors for the five main LULC spatial patterns at five individual time nodes were calculated. Then, the multiyear average values of the q statistic over five different time nodes were computed for analysis to partially eliminate the influence of data uncertainty. The other was the attribution analysis of the major LULC change types in the SRB from 2000 to 2018, namely, the q statistic of eleven factors for the nine major LULC change types were calculated.

The risk detector can not only be utilized to evaluate whether there is a significant difference in the mean value of the dependent variable between two levels of a factor, but also to obtain the mean value of the dependent variable at each level of a factor. In this study, we adopted the risk detector to determine the mean area of every kind of LULC change at different levels of its main drivers to assess the correlations between the driving factors and the corresponding LULC change categories. All of the above attribution analyses were first conducted in ArcGIS, which stacked layers of all variables in advance and collected the values of the dependent and independent variables in each grid cell of the research area through the sampling tool. Then, the collected information was exported into Excel to run the GeoDetector model and obtain the attribution analysis results.

4. Results

4.1. LULC Patterns and the Driving Forces in the SRB

4.1.1. The Composition Structure and Spatial Distribution Patterns of LULC in the SRB

Figure 3f illustrates that, from 2000 to 2018, the LULC of the SRB mainly consisted of four categories: grassland, bare land, cropland, and forest. The mean areas of these categories in the last two decades accounted for 57.48%, 23.91%, 13.17%, and 5.19% of the entire basin, respectively, whereas the proportions of settlements and others were relatively small, accounting for only 0.15% and 0.10%.

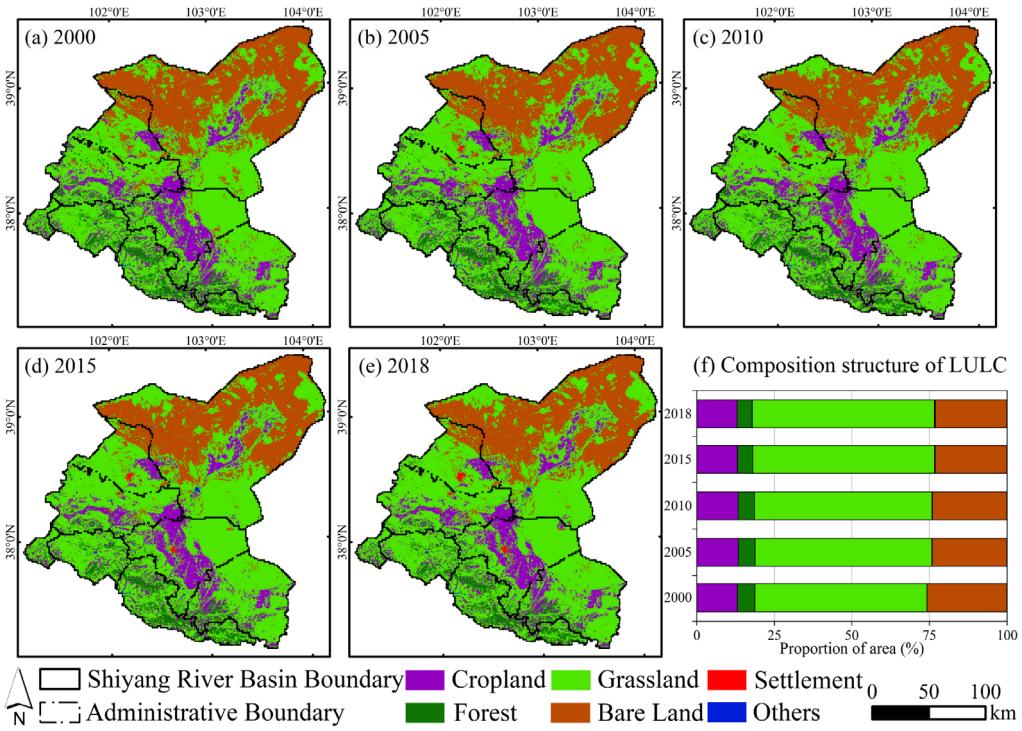

Figure 3. LULC patterns (**a**–**e**) and composition structure of LULC in the SRB (**f**) from 2000 to 2018.

Grassland, the dominant LULC type in the SRB, was broadly distributed in the basin, but was primarily concentrated in the upstream mountainous area and the middle reaches (Figure 3a–e). The most considerable LULC in the downstream areas of the basin was bare land, which was distributed in Minqin County and Jinchuan District. Only small areas of bare land were sporadically distributed in other parts of the basin. As the third-largest landscape of the basin, cropland was primarily distributed in the middle reaches of the basin, which was just below the upstream river outlet. Additionally, cropland was generally distributed close to the banks along the river. The distribution of forest area was more concentrated upstream with high elevation. In contrast, settlements were distributed in the middle and lower reaches, forming a point-like distribution. Since the LULC type of others was mainly composed of permanent snow and ice and water bodies, it was sporadically distributed in the mountainous upper and middle reaches of the basin.

4.1.2. Driving Forces behind LULC Patterns in the SRB

Figure 4a–e illustrates that the main driving forces behind the distribution patterns of various LULC types differed. Generally, the distributions of cropland and settlements were chiefly affected by topography (mainly the distance to urban and township centers) and human activities. Various natural and anthropic factors drove the spatial patterns of the forest, grassland, and bare land.

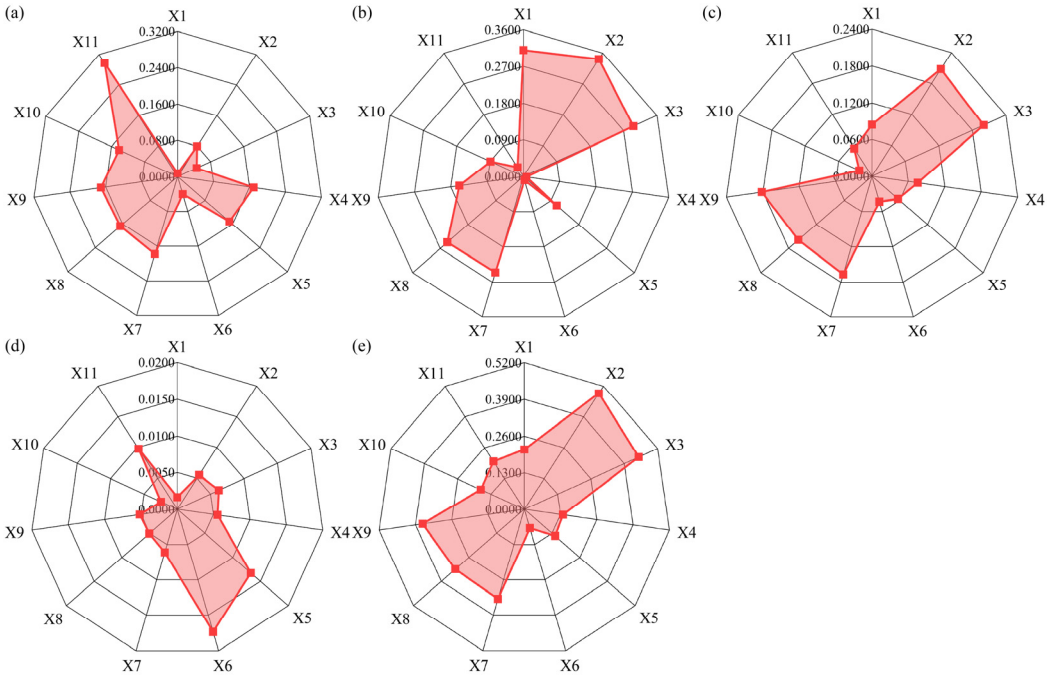

Figure 4. Driving forces behind the spatial distribution patterns of five primary LULC categories in the SRB during 2000–2018: (**a**) cropland, (**b**) forest, (**c**) grassland, (**d**) settlement, and (**e**) bare land. Notes: The explanatory power of each factor in this figure was the multiyear mean value of the *q* statistics from 2000 to 2018. The *q* statistic of each factor in each year passed the significance test. The factor codes are as follows: X1, temperature; X2, precipitation; X3, altitude; X4, population density; X5, GDP; X6, GDP per capita; X7, total water consumption; X8, surface water supply; X9, groundwater supply; X10, distance to the rivers; and X11, distance to urban and township centers. The definitions of each factor are detailed in Table 1.

During the whole study period, the distance to urban and township centers exhibited the most substantial explanation for the spatial pattern of cropland (29.73%) (Figure 4a). The explanatory powers of GDP, GDP per capita, total water consumption, surface water supply, groundwater supply, and distance to the rivers were all approximately 16%. The

other factors could only explain less than 10% of the cropland distribution. The explanatory power of temperature was the lowest, at only 0.75%. The explanatory power of each factor for the spatial distribution of settlements was lower than that of the other four main LULC categories (Figure 4d). The two largest multiyear average q values were from economic factors (GDP and GDP per capita), which provided the strongest explanation for settlement distribution. The explanatory power of distance to urban and township centers ranked third to the economic factors, and other factors explained approximately 0.5% or less. As shown in Figure 4b, climatic factors and elevation were demonstrated to be more vital for the forest distribution pattern, whose mean annual q statistics were all greater than 30%.

In contrast, the explanatory powers of population density, GDP per capita, distance to the rivers, and distance to urban and township centers were all below 10%, especially for population density and GDP per capita, whose mean annual q statistics were all less than 1%. The main driving factors for the grassland distribution were precipitation, DEM, total water consumption, surface water supply, and groundwater supply, whose explanatory powers ranged between 15% and 20%. Additionally, all the q values of the other factors were less than 10%. For the distribution of bare land (Figure 4e), the two factors that had the most significant impact were the annual mean precipitation (48.93%) and elevation (44.66%). The explanatory powers of total water consumption, surface water supply, and groundwater supply ranged from approximately 30% to 35%. Nevertheless, GDP per capita affected the bare land spatial pattern the least (7%).

4.2. LULC Change and its Driving Forces in the SRB

4.2.1. LULC Change in the SRB during 2000–2018

1. Temporal Variations in the Areas of LULC in the SRB

In general, the area of all LULC categories presented either a monotonic increasing or decreasing variation trend, except for the cropland. The variation in cropland initially showed an increasing trend (2000–2005) and then decreased (2010–2018) throughout the entire study period (see Appendix C: Table A2). According to the analysis of the MK test, the area variations in forest, grassland, settlement, bare land, and others passed the significance test with a confidence level of 95%, showing significant growths or reductions.

Regarding the five primary LULC types of cropland, forests, grassland, bare land, and settlements in the SRB, grassland and bare land exhibited the most significant variations during 2000–2018. Grassland grew by 1291.32 km^2 and bare land declined by 1052.64 km^2 (Table A2). Settlements had the highest rate of change, increasing approximately sixfold between 2000 and 2018. In contrast, cropland exhibited the lowest rate of change (−0.53%). Furthermore, the cropland area varied the least among the five main LULC categories in the SRB, decreasing by 27.36 km^2.

2. Spatiotemporal Patterns of the Main LULC Change Types in the SRB

Figures 5 and 6 illustrate the LULC changes in the SRB from 2000 to 2018. Throughout the whole study period, the main types of LULC change were (1) the mutual conversions among cropland, grassland, and bare land; (2) the transformation from forest to grassland; and (3) the expansion of settlements.

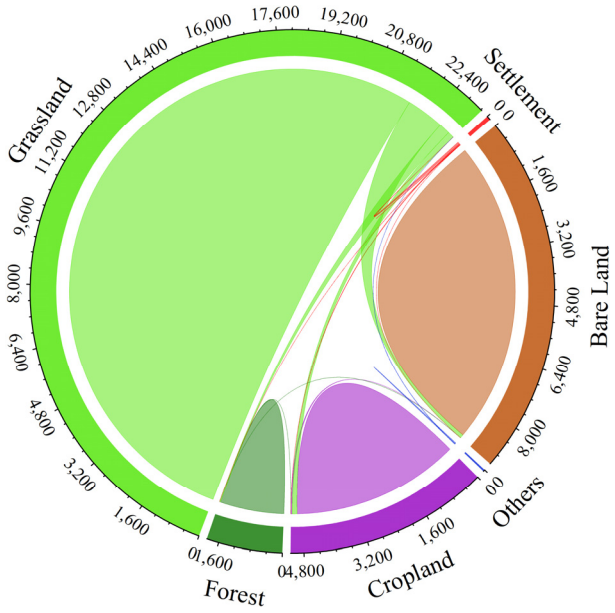

Figure 5. LULC changes in the SRB from 2000 to 2018 (unit: km²). Notes: The arcs represent the area of each LULC category in the SRB during 2000–2018 after land use conversion had occurred. The connecting lines show the conversion relationship among various LULC categories. The color of the connecting line between two LULC categories indicates which LULC type has a higher proportion in the transformation. For example, the connecting line between grassland and bare land is illustrated with the color of grassland, indicating that the area transferred into grassland was larger. The thickness of the connecting line indicates the size of converted area between two LULC types; a thicker line indicates a greater conversion area between two LULC types.

From 2000 to 2018, the growth of cropland was mainly induced by the reclamation of grassland and bare land, accounting for 77.56% and 22.29%, respectively (Figure 6). This chiefly occurred in the middle and lower reaches of the SRB (Figure 7). Among them, 73.93% of the increase mainly happened in 2000–2005, which was the stage where the cropland showed a significant increase (Table A2). Grassland was the LULC category to which most of the cropland was converted, accounting for 88.85% of the cropland conversion (Figure 6). It was sporadically distributed in the upper and middle reaches (Figure 7). A considerable net decline in cropland had occurred since 2005, dominated by the growth of grassland (accounting for nearly 93% of the cropland loss) (Table A2). The significant reduction in cropland after 2005 was probably related to the performance of the Key Treatment Program of the Shiyang River Basin in 2007. One of the critical objectives of this program was to reduce agricultural water consumption by reducing unreasonable cropland, thereby protecting the basin's environment [47].

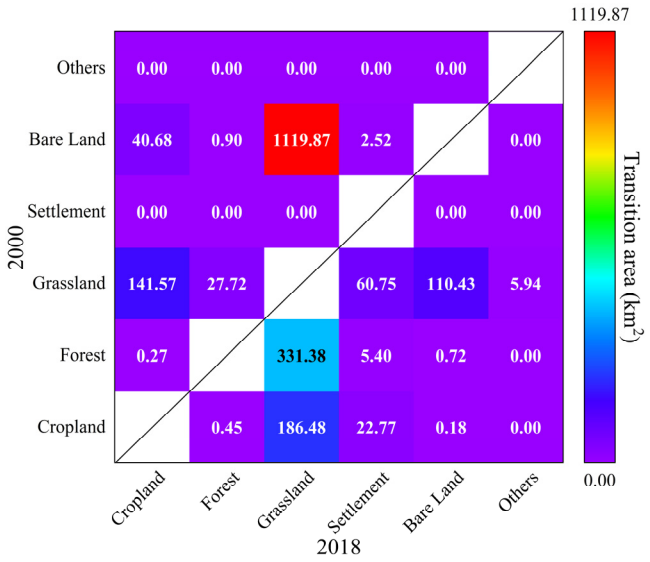

Figure 6. Land use transfer matrix of the SRB during 2000–2018.

The mutual conversion of grassland and bare land was the most significant LULC change type in the SRB. From 2000 to 2018, the net increase in grassland area was 1291.32 km². Approximately 78% came from the decline in bare land (Figure 6). This mainly occurred during 2000–2005 (Table A2), which might be because this period was immediately after the initiation of the Grain for Green Project. The transformation from bare land to grassland was mainly distributed sporadically in the middle and lower reaches of the basin, chiefly distributed on the east and west sides of the basin near the edges of the Badain Jaran Desert and the Tengger Desert (Figure 7). Moreover, forest loss was another major contribution to grassland growth. This mainly occurred in the upper and middle reaches of the SRB (Figure 6; Figure 7). In terms of bare land, although its area reduced significantly during the entire study period, some grassland was still converted to bare land. The conversion area was about 110.43 km², and nearly half occurred between 2005 and 2010 (Figure 6; Table A2). This was broadly distributed on the edges of the Minqin Oasis, in the lower reaches of the Shiyang River (Figure 7).

The settlement area mainly expanded by encroaching into grassland and cropland (Figure 6). In the past two decades, the settlement areas in the SRB increased by 91.44 km²; its rate of increase was relatively consistent in each period (Table A2). Additionally, the loss of grassland and cropland accounted for approximately 66% and 25% of the total settlement increase, respectively (Figure 6). This demonstrated the characteristics of concentration distribution in the urban centers, which indicated that the mechanism of urbanization progression in the SRB was mainly based on point-like diffusion (Figure 7).

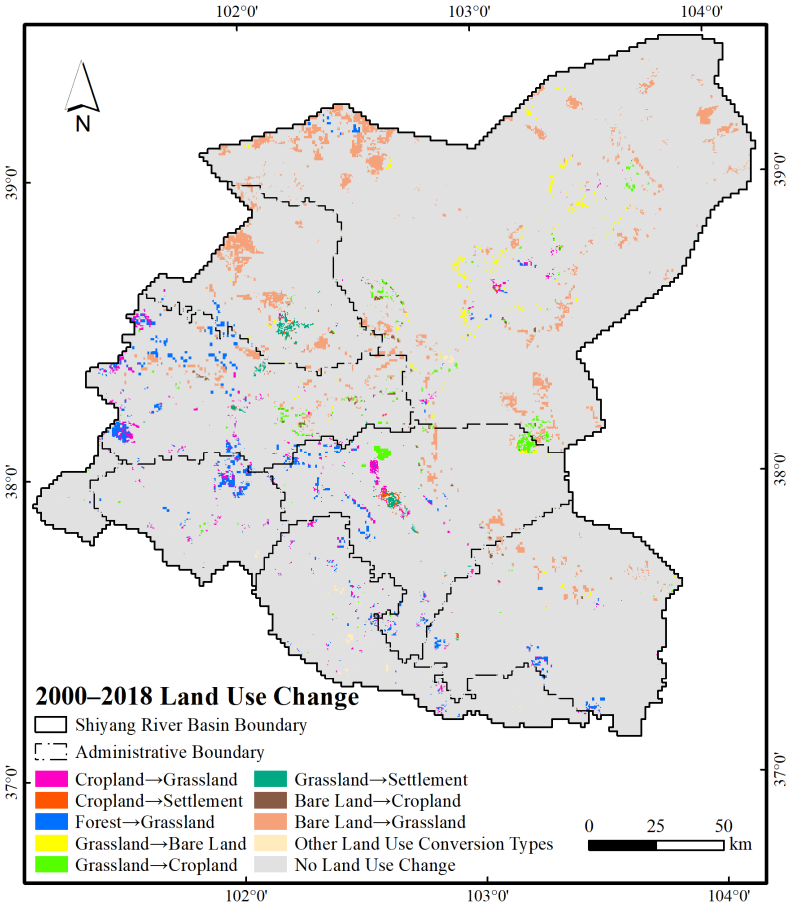

Figure 7. Spatial pattern of LULC changes in the SRB during 2000–2018.

4.2.2. Driving Force Variations in LULC Changes in the SRB

The variation in each factor during the study period presented different spatiotemporal characteristics (see Appendix D: Figure A2). Throughout the entire study period, the temperature in the northeast of the research region increased the most, and the temperature amplitude gradually declined from northeast to southwest. The precipitation increased mainly in the southeastern regions, whereas it significantly decreased in the southwest. Population density, GDP, and surface water supply increased considerably in the areas surrounding the Liangzhou District. Moreover, higher GDP growth per capita mainly occurred in Jinchuan and Sunan. Areas with significant decreases in total water consumption and groundwater supply were mainly situated around Liangzhou. In addition, the increases in total water consumption and groundwater supply chiefly occurred in Jinchuan and Yongchang.

1. Driving Forces behind the Main LULC Changes in the SRB

According to the factor detection results, the main driving factors behind different LULC types converted to the same LULC type were generally the same as in the SRB (Figure 8; Appendix E: Table A3). Total water consumption, GDP, and distance to urban and township centers considerably impacted the conversion of cropland and grassland to settlements, indicating that they were mainly affected by anthropogenic activities (Figure 8b,f).

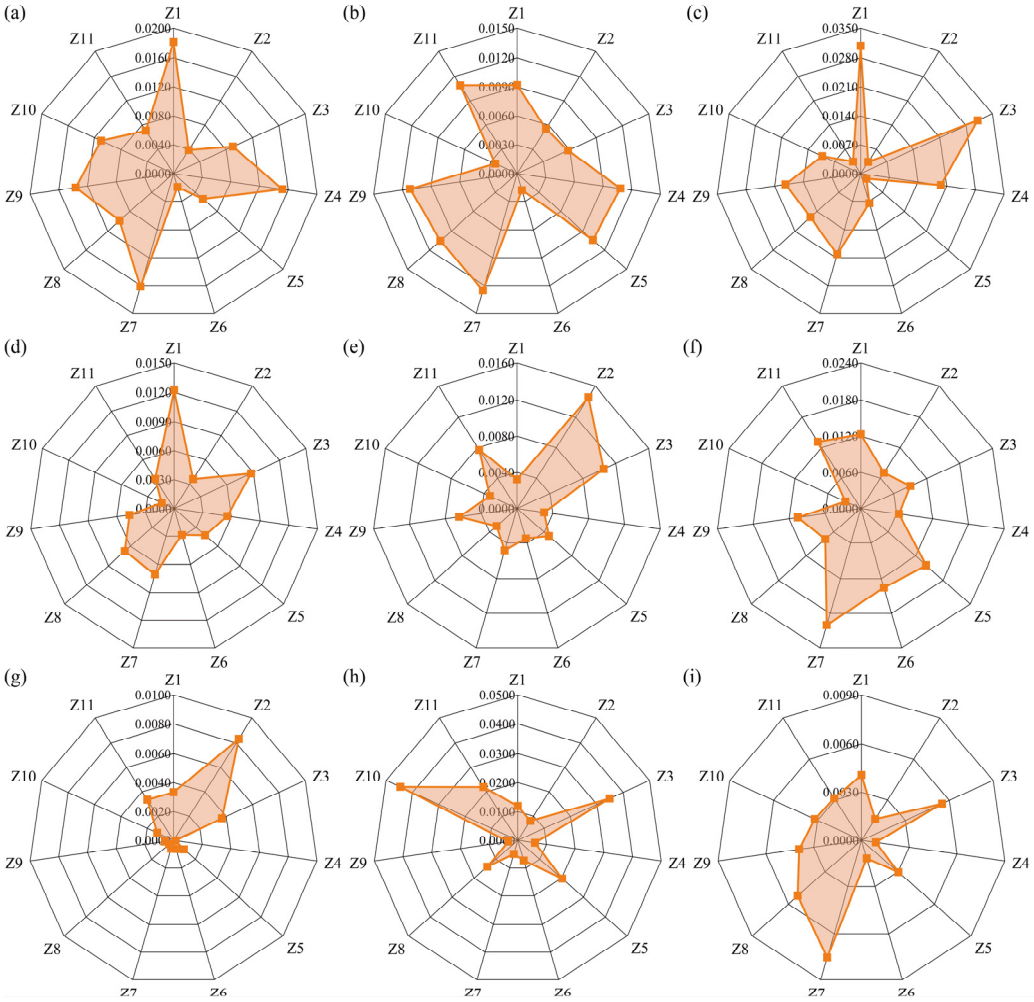

Figure 8. Driving forces behind LULC changes in the SRB during 2000–2018: (**a**) cropland→grassland; (**b**) cropland→settlement; (**c**) forest→grassland; (**d**) grassland→bare land; (**e**) grassland→cropland; (**f**) grassland→settlement; (**g**) bare land→cropland; (**h**) bare land→grassland; and (**i**) other land use conversion types. Notes: The factors in this figure indicate the variation in each factor between 2000 and 2018. The factor codes are as follows: Z1, temperature; Z2, precipitation; Z3, altitude; Z4, population density; Z5, GDP; Z6, GDP per capita; Z7, total water consumption; Z8, surface water supply; Z9, groundwater supply; Z10, distance to the rivers; and Z11, distance to urban and township centers. The meaning of each factor is detailed in Table 2.

The explanatory power of each factor for the conversion of grassland and bare land to cropland was similar; both were mainly affected by DEM, distance to urban and township centers, and precipitation variation. It manifested that the conversions to cropland were not only affected by humans but were closely connected to climate change and topography (Figure 8e,g). Anthropic and climatic factors chiefly influenced the transformation from grassland to bare land. The major driving factors were temperature change, total water consumption variation, surface water supply variation, and altitude differentiation (Figure 8d). The changes in temperature, population density, and total water consumption had significant impacts on the transformations of cropland and forest into grassland (Figure 8a,c). Furthermore, terrain factors dominated the transformation from bare land to grassland, namely, the elevation, distance to the rivers, and distance to urban and township centers.

2. Differences in Driving Factor Influences on LULC Change at their Levels

Figure 9 depicts the risk detector results, showing that the degree of LULC change varied among different levels of driving factors. The areas of different land conversions

into the same LULC type had similar distribution patterns at different levels of their main driving factors. This further proved that the driving forces behind various LULC types that transferred into identical LULC types were generally the same in the SRB.

The degree of settlement expansion presented a growing trend with the increase in GDP growth and the decrease in distance to urban and township centers. It indicated that settlement expansion was closely related to the rapid growth of the urban economy (Figure 9a). In the regions where the GDP growth exceeded CNY 1.28 million, the cropland and grassland converted into settlements were 17.37 km² and 47.88 km², respectively, accounting for about 77% of the overall conversion area of each. The cropland conversion to settlement fully occurred within 5.8 km from the urban and township centers (Figure 9c). Moreover, over 90% of the grassland conversion to settlement was concentrated within the same distance. The vast majority of farmland and grassland occupied by settlements were distributed in the regions where water consumption decreased and increased significantly (Figure 9b).

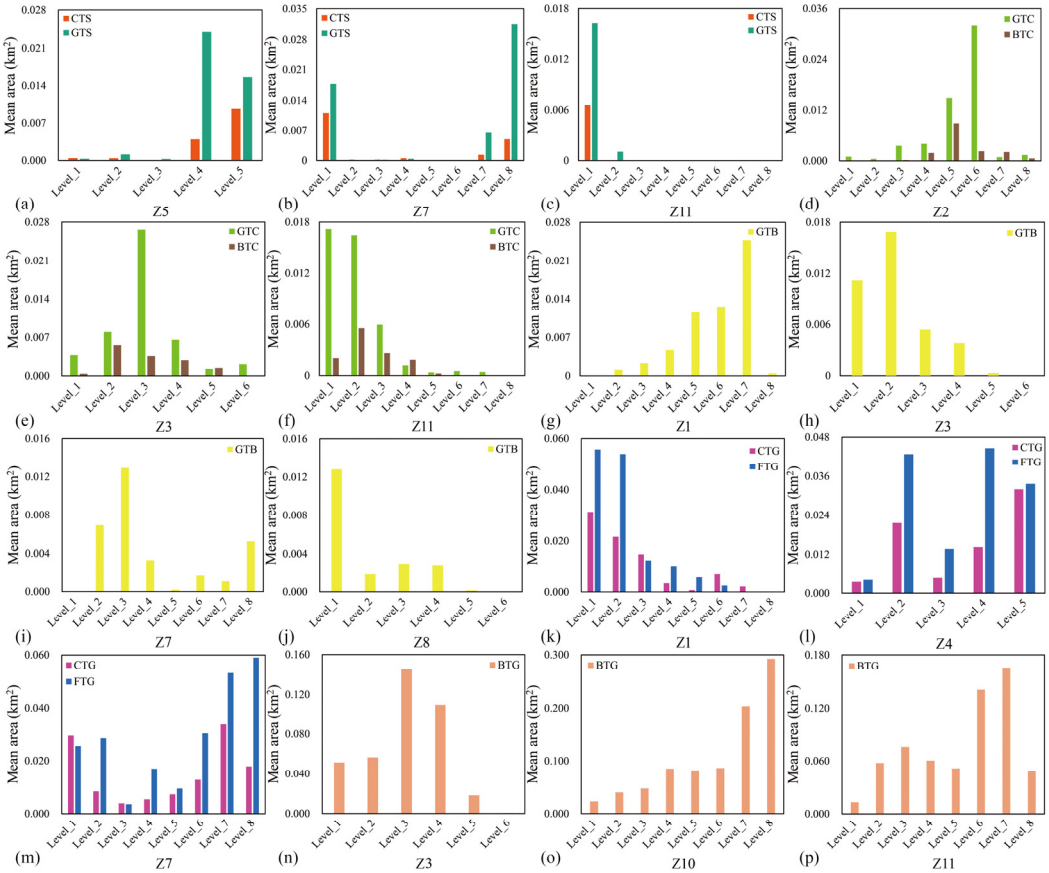

Figure 9. Variations in the influence of driving factors on LULC changes at different levels: (**a–c**) mean areas of cropland/grassland converted to settlement at different levels of the main driving factors; (**d–f**) mean areas of grassland/bare land converted to cropland at different levels of the main driving factors; (**g–j**) mean areas of grassland converted to bare land at different levels of the main driving factors; (**k–m**) mean areas of cropland/forest converted to grassland at different levels of the main driving factors; (**n–p**) mean areas of bare land converted to grassland at different levels of the main driving factors. Notes: The levels represent the strata of factors generated by discretization; the discretization methods and the values of factors corresponding to each level are shown in Table A4 in Appendix F. The factor codes are as follows: CTG, cropland→grassland; CTS, cropland→settlement; FTG, forest→grassland; GTB, grassland→bare land; GTC, grassland→cropland; GTS, grassland→settlement; BTC, bare land→cropland; BTG, bare land→grassland; OTS, other land use conversion types; Z1, temperature; Z2, precipitation; Z3, altitude; Z4, population density; Z5, GDP; Z6, GDP per capita; Z7, total water consumption; Z8, surface water supply; Z9, groundwater supply; Z10, distance to the rivers; and Z11, distance to urban and township centers. The meaning of each factor is presented in Table 2.

According to the results of the two categories of land use transformation to cropland, with the increases in precipitation and elevation, the areas of grassland and bare land that transformed to cropland increased first and then decreased (Figure 9d,e). Concretely, approximately 77.69% and 71.24% of the grassland and bare land conversion to cropland were distributed in the regions with precipitation growths of 39.37–79.09 mm, respectively (Figure 9d). In the region with an altitude of 1439–1579 m, the area of grassland converted to cropland was the greatest, reaching 78.03 km^2. Meanwhile, the maximum conversion area of bare land to cropland was mainly located in the area where the elevation was 1350–1439 m (Figure 9e). However, the conversion area distributions of those two LULC changes slightly differed in terms of the distance to urban and township centers. As the distance to urban and township centers grew, the grassland area converted to cropland gradually reduced. The transformations mainly occurred within 10.36 km from the urban and township centers, accounting for 83.41% of the total conversion area (Figure 9f). For the transformation of bare land to cropland, the transformation area increased at first and then decreased with the increasing distance from urban and township centers (Figure 9f). It was concentrated the most in the regions 5.82–10.36 km away from the cities and towns, covering approximately 19.62 km^2.

For the transformation from grassland to bare land, generally, with the gradual rise in temperature and decrease in surface water supply, the impacts of these two driving factors were gradually enhanced (Figure 9g,j). The conversion area of bare land increased first and then reduced with the gradual increase in elevation (Figure 9h). The conversion area peaked when the altitude ranged between 1350 and 1439 m. Furthermore, approximately 82.31% of the conversion area was distributed where the total water consumption had fallen by 0.12–0.20 billion m^3 (Figure 9i).

Furthermore, for the three LULC change types converted to grassland, the cropland and forest conversion areas were distributed similarly at various levels of their main driving factors (Figure 9k–m). Specifically, as the temperature rose, the area converted to grassland gradually reduced (Figure 9k). The cropland and forest conversion areas in the regions with a temperature variation range of −0.01 to 0.16 °C were 117.81 km^2 and 248.22 km^2, respectively, accounting for approximately 63.18% and 74.90% of each total transformation area. The influence of population factors on those two conversions generally increased with the growth in population density (Figure 9l). However, in the areas with a population density variation of −0.78 to 2.38 people per km^2, the average areas of cropland and forest conversion were relatively larger, reaching 0.02 km^2 and 0.04 km^2, respectively. Additionally, the effects of total water consumption on these two LULC change types showed a rising trend and then fell (Figure 9m). The conversions mainly occurred in the regions where the total water consumption exhibited a significant decline and considerable growth.

With the increases in distance to the rivers and towns, the impacts of these two factors on the transformation from bare land to grassland gradually increased (Figure 9o). In contrast, the influence of altitude rose first and then reduced as it increased (Figure 9n). In the areas with an elevation of 1439–1579 m, the mean conversion area reached its maximum, at approximately 0.15 km^2.

5. Discussion

5.1. Driving Mechanisms behind the Formation of and Changes in LULC Patterns

5.1.1. Driving Mechanisms behind the Formation of LULC Patterns

For endorheic river basins, artificial oases represent key concentrations of anthropogenic activities and chiefly consist of cropland and settlements. Generally, economic activities require vast infrastructure construction as hardware support to ensure economic development [48], such as factories, shopping malls, railway stations, etc. In turn, the development of economic activities boosts infrastructure construction. Therefore, because

settlements contain these infrastructures, their spatial patterns are closely related to economic factors, which is consistent with some previous research [4,17,49].

On the other hand, the SRB is one of China's crucial commodity grain bases [22]. The development of agriculture not only guarantees the food security of the basin or even the whole country, but also plays a vital role in the economic development of the basin. Additionally, approximately 90% of the population in the SRB is concentrated in the hinterland of artificial oases such as Liangzhou, Jinchuan, and Minqin. Hence, agricultural activities are mainly carried out in artificial oases with convenient transportation, a large population, and a developed economy. More importantly, due to the water shortages in arid regions, internal farming activities primarily rely on irrigation through artificial canals or other water conservancy facilities. Considering the construction cost of irrigation facilities as well as the cost and efficiency of water conveyance, the cropland in the SRB was mainly distributed in the vicinity of cities and towns.

Water is the most critical element affecting vegetation growth and distribution in arid inland regions [50,51]. In the SRB, precipitation is primarily concentrated in the upstream mountainous areas. Sufficient rainfall is beneficial to the growth of forests and grassland. From the middle reaches to downstream, the gradual temperature increase, and the decrease in precipitation lead to increased evaporation, and the availability of water became smaller. Thus, the grassland distribution gradually decreases, and the area of bare land rises.

Furthermore, a considerable part of the grassland was distributed in the middle and lower reaches with relatively little rainfall. This part of the grassland survived more by absorbing shallow groundwater [52]. However, high-intensity anthropogenic activities in these regions have seriously affected the local hydrological regime [53,54], resulting in fluctuations in surface runoff and groundwater levels, which strongly affect the growth of the surrounding natural vegetation [55]. Therefore, the degree of water resources utilized in the SRB affected vegetation growth to a large extent. Additionally, this was the main reason that the impact of water utilization on grassland and bare land distribution was more significant than that on the forests.

In conclusion, the formation of land use patterns in the SRB was not driven or constrained by a single driving factor, but by various factors interconnectedly and jointly affecting the spatial distribution of LULC.

5.1.2. Driving Mechanisms behind LULC Changes

Over the past two decades, the ecology of the SRB has generally improved. A large amount of bare land and cropland has been used to restore vegetation. However, unreasonable LULC exploitation still existed in the basin, resulting in the basin facing potential ecological risks in some areas. For instance, rapid urbanization mainly occurred through occupying the grassland and cropland; degradation existed in the forests and some of the grassland. These conclusions were consistent with previous studies [11,51,56–58].

Concretely, a large area of vegetation recovered in the bare land was the main reason for the ecological improvements in the SRB. Altitude and proximity factors were the main reasons for this improvement. Li et al. suggested that the proximity factors can directly reflect the intensity of anthropogenic activities and profoundly affect LULC changes [59]. Therefore, the ecological restoration of bare land might be partially due to the reduction in groundwater wells and the operation of the ecological water transport project since the operation of the Key Treatment Program of the Shiyang River Basin in 2007. These countermeasures elevated the groundwater levels near the towns, promoting natural vegetation restoration, such as the Huang'antan Enclosed Conservation Area near Jiahe Township in Minqin County and the terminal lake (Qingtu Lake). These areas were mainly distributed within 5.8–15.2 km away from the towns [60,61]. In addition, in 2011, the local government planned and implemented the "Prevention and Control of Desertification and Ecological Restoration Plan". It suggested that local governments should strengthen the construction of ecological function zones in the desert–oasis transition zones of the

northern and western parts of the SRB to achieve comprehensive ecological improvements and prevent the further erosion of farmland and settlements by wind and sand. As a result, in recent years, large-scale artificial greening has been carried out in some regions close to the edge of deserts, relatively far from rivers and towns [61–63]. In short, with the guidance of policies and the regulation of ecological restoration projects, large-scale grassland growth could substantially help restore the fragile ecological environment and enhance the ecosystem service function of the SRB.

During the past two decades, the Western Development Strategy, enacted by the Chinese government in 2000, has vastly boosted the urbanization of the SRB [17,64]. This policy implementation brought rapid population growth and increased the demand for housing and the expansion of enterprise scales. The rapidly growing economy could satisfy the investment and construction of housing, factories, and other infrastructure, further addressing the land demand brought by urbanization expansion, and thus promoting settlement expansion. However, urbanization in the SRB has rarely been conducted through bare land development, only expanding outward from the original urban region by occupying original cropland and grassland around the towns. This kind of extension mode has caused evident damage to the surrounding natural vegetation. Without rational regulation, it may cause further harm to the ecological environment near the cities and towns in the future.

Another land use conversion which might cause ecological problems in the SRB was the reduction in forests and part of the grassland. The degeneration of the forests had chiefly occurred in the upstream mountainous areas, which have had small population density growth and increased water consumption. This variation might be because the upstream Qilian Mountains in the national nature reserve are rich in natural resources and cultural landscapes. Before 2015, the tourism industry in the Qilian Mountains had developed rapidly, receiving more than 0.3 million tourists per year on average. Numerous tourism facilities were built in scenic areas, leading to extensive forest deforestation [65]. Although the Chinese government has vigorously remedied the ecological problems in the Qilian Mountains since 2018, it still needs some time to recover.

Additionally, most grassland deterioration happened in downstream Minqin County (Figure 7). The soil texture of the downstream desert was mainly sandy soil with high porosity and good permeability; thus, temperature rises cause increased evaporation, leading to declining groundwater levels and, eventually, the death of some vegetation. The result was consistent with the previous research [51,57,58].

On the other hand, to restore and protect the ecological environment of the SRB, locals have taken many measures to realize these goals, including returning the cropland to green land. However, most of the transformations occurred in the upper and middle reaches. Many farmers in the lower reaches believe that reducing farmland would affect their income, so they were not very supportive of the cropland-reducing policy [66–68]. Moreover, the local administration also actively adjusted the local agricultural structure and increased the construction of greenhouses [51]. They also promoted water-saving irrigation technology to convert some farmland from traditional irrigation means, such as flood and border irrigation, to pipe and drip irrigation. This shift effectively reduced the agricultural water consumption and loss of surface water delivery in Minqin. All these governing measures were conducive to increasing runoff downstream and improving the ecology of the lower reaches [69,70]. However, as the irrigation means change, the reduction in water consumption will also significantly reduce the amount of lateral seepage water around the irrigation canals [71]. According to Cao et al., the groundwater depth in the western Minqin Oasis was more than 12 m. When the groundwater depth exceeded 4 m, the vegetation growth mainly depended on the surface soil moisture [60,72]. Considering the low annual accumulated precipitation in Minqin, the natural vegetation near the towns in western Minqin Oasis was likely to grow through the seepage water derived from the traditional irrigation modes.

Thus, the promotion and utilization of water-saving irrigation have improved the efficiency of regional water utilization and reduced the waste of water resources. However, the transformation of irrigation modes also caused the degradation and death of some original natural shelterbelts and vegetation which relied on the seepage of water from traditional irrigation practices. This is an example of an ecological effect caused by converting traditional irrigation to water-saving irrigation [69,71,73]. Without scientific and reasonable control, it might threaten the surrounding agricultural production activities and the ecological environment, which should draw decision-makers' attention.

5.2. Suggestions for LULC Planning in the SRB

In early 2021, the Chinese government issued the Fourteenth Five-Year Plan, which stated that by 2035, China would achieve multiple goals, such as new industrialization, informatization, urbanization, and agricultural modernization [74]. It pointed out that it was necessary to optimize the spatial patterns of the land and gradually develop three spatial patterns with urbanization areas, key agricultural production areas, and ecological function areas based on the carrying capacity of the environment and resources. Therefore, analyzing the evolution process of regional LULC spatial distribution and clarifying the driving factors behind LULC patterns and LULC changes are essential for promoting the sustainable development of society, the economy, and the environment. Based on the results of this research, we propose the subsequent suggestions for the decision-makers to optimize the spatial distribution of land use of the SRB in the future.

(1) Promoting urbanization appropriately. "People-oriented" is the prerequisite for human social development. Therefore, appropriate and necessary urbanization benefits socioeconomic development, ecosystem service protection, and the improvement of people's living standards [21]. However, the scale and rate of settlement growth should be controlled, and locals should pay attention to the efficiency of urban space utilization. Meanwhile, sufficient urban ecological land should be reserved, which could be considered ecological compensation for the destruction of surrounding natural green space caused by urban expansion. In summary, ecological damage should be minimized during urbanization.

(2) Protecting elemental cropland and improving production efficiency. With the development of urbanization and the operation of ecological restoration schemes, cropland has reduced in the SRB over the past few decades. Excessive reductions in cropland may threaten regional food security to some extent. Consequently, the quantity of elemental cropland should be fully guaranteed to ensure essential ecological environment health and meet appropriate and necessary urbanization construction. In addition, the cropland's spatial pattern should be optimized, considering the ecological functions of different regions. For instance, agricultural activities should be avoided as much as possible in the upper reaches, which are crucial water conservation areas of the SRB. Instead, they can be appropriately shifted to the middle and lower reaches. In addition, it is necessary to continuously improve the structure of the agricultural industry and promote water-saving irrigation, which is suitable for local regions. However, people should focus on ecological problems, such as the degradation of natural shelterbelts around cropland caused by the change in irrigation means. Relevant investigations, assessments, and remedial plans should be developed before water-saving irrigation techniques are used, which could avoid secondary damage to the local ecological environment in the short term.

(3) Protecting ecological land. Vegetation is a significant natural barrier to ensure regional ecological security and prevent desertification in arid inland regions. Hence, people should continue to increase forests and grassland in the basin under the guidance of relevant ecological environment protection policies. Additionally, relevant laws and regulations should be established to prevent the recurrence of severe ecological damage. For example, given forest degradation upstream, artificial planting

could be adopted to accelerate forest recovery, and corresponding nature reserves should be established. Nevertheless, blind planting must be restricted, and the government should plan the planting area, layout, and varieties scientifically and rationally to avoid the unnecessary consumption of water resources.

5.3. Limitations and Future Work

There were some limitations to this research. Due to the limitation of data availability, we did not consider the difference in soil type as one of the potential driving factors. Additionally, because the preclassified products of ESA were selected as the land use data, specific errors were inevitable in the classification process. Meanwhile, for some areas with low vegetation coverage, different studies have classified them into various categories. In this study, we reclassified shrubs and some land covers with low vegetation coverage into grassland, which may have lost part of the land cover information, resulting in certain deviations between our results and other previous studies. In addition, because the GeoDetector analysis was based on grid cells, the results will be affected by the grid size and discretization methods to some extent. The area of this study was relatively small, and the impact of those two effects was primarily considered in previous studies with large study areas [31]. Moreover, to date, there is no optimal criterion for selecting grid size and discretization method; therefore, in this study, evaluations of the effect of grid size and discretization method were not taken into consideration. We will consider it in future research.

In the next stage, we will consider dividing the SRB into different ecohydrological function zones and try to optimize and predict the land use patterns in the SRB by analyzing and calculating the water requirements and consumption of different land uses on the premise of ensuring the main ecological objectives of the basin.

6. Conclusions

In this study, land use transfer matrices and a geographic detector were employed to reveal the evolution of LULC patterns and the driving forces behind the formation of and changes in LULC in the SRB. The results revealed that grassland and bare land were the two most extensive LULC types. Anthropogenic activities were the main driving factors influencing the spatial patterns of cropland and settlements distributed in the middle and lower reaches of the basin. For the forest, grassland, and bare land, their spatial distributions were all chiefly impacted by the joint influence of natural and anthropic factors.

In the past 18 years, the LULC patterns in the SRB have changed significantly. Grassland and settlements presented a rising tendency. In contrast, the areas of cropland, forest, and bare land have decreased. With the implementation of the Key Treatment Program of the Shiyang River Basin, cropland demonstrated a variable trend of first increasing and then declining after 2005. The major LULC changes in the SRB were the mutual conversions among cropland, grassland, and bare land. Moreover, approximately 91% of the settlement expansion derived from the occupation of cropland and grassland. The decline in forest area was mainly because of its conversion to grassland, which generally occurred in the Qilian Mountains and its surroundings.

Climate change, socioeconomic variation, topographical factors, and changes in development policies all drove LULC changes in the SRB; however, the primary driving force depended on specific LULC changes. The main driving factors of different LULC conversions to the same LULC type were similar in the SRB. The transformation of bare land to grassland was chiefly affected by the elevation and proximity factors. The expansions of settlements, characterized by the occupation of grassland and cropland, were mainly driven by the distance to urban and township centers, economic growth, and variations in total water consumption. Variations in anthropogenic and natural factors both caused degradation of the forests and grassland. There were apparent variations in the impacts of the driving factors on the LULC changes at their different levels.

Facing the continuous changing climate conditions and the rapid development of society, land use managers and planners should continuously update and improve their LULC plans and strategies in a timely manner, according to the driving forces behind the current LULC patterns and changes. This will ensure the sustainable and rational use of land resources and may be conducive to achieving sustainable development. The results obtained in this paper could, to a certain extent, fill the gap in the quantitative driving analysis of LULC pattern formation and changes in the SRB. Furthermore, it could afford a scientific framework reference for the driving analysis of LULC in other arid endorheic river basins worldwide. Further research would address the optimization and prediction of LULC, with consideration towards distinguishing ecohydrological function zones.

Author Contributions: Conceptualization, X.C.; formal analysis, J.L.; data curation, J.L.; writing—original draft preparation, J.L.; writing—review and editing, X.C. and F.H. All authors have read and agreed to the published version of the manuscript.

Funding: This research received no external funding.

Institutional Review Board Statement: Not applicable.

Informed Consent Statement: Not applicable.

Data Availability Statement: Not applicable.

Conflicts of Interest: The authors declare no conflicts of interest.

Appendix A

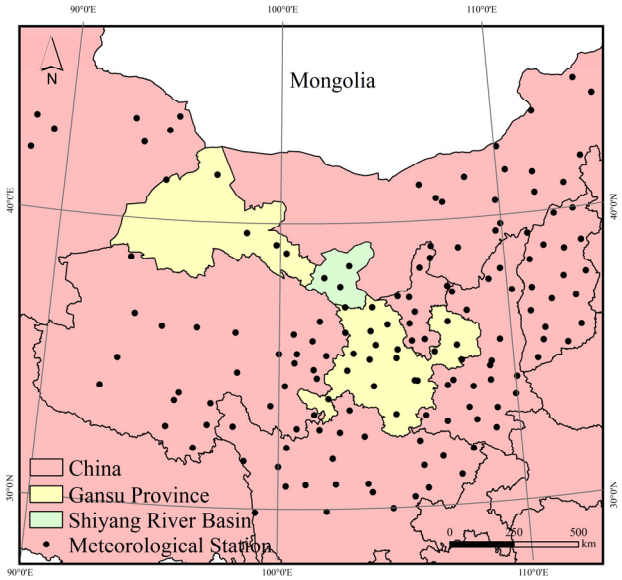

Figure A1. Distribution of weather stations surrounding the Shiyang River Basin (SRB).

Appendix B

Table A1. Discretization methods and the 11 potential driving factors of the formation of and main changes in LULC in the SRB.

Factor	Method	Level Numbers	Unit
X1, Z1	Natural Breaks	8	°C
X2, Z2	Natural Breaks	8	mm
X3, Z3	Quantile	6	m
X4, Z4	Natural Breaks	5	persons/km^2
X5, Z5	Natural Breaks	5	10^4 CNY/ km^2
X6, Z6	Natural Breaks	5	10^4 CNY/ km^2
X7, Z7	Natural Breaks	8	10^8 m^3/ km^2
X8, Z8	Natural Breaks	6	10^8 m^3/ km^2
X9, Z9	Natural Breaks	6	10^8 m^3/ km^2
X10, Z10	Natural Breaks	8	km
X11, Z11	Natural Breaks	8	km

Notes: The definitions and descriptions of factors are shown in Tables 1 and 2 in the manuscript.

Appendix C

Table A2. Land use transfer matrices of different periods from 2000 to 2018 in the SRB (unit: km^2).

		2005						
	Land Use Types	**Cropland**	**Forest**	**Grassland**	**Settlement**	**Bare Land**	**Others**	**Total Area**
2000	Cropland	5142.78	0.09	12.51	2.97	0.00	0.00	5158.35
	Forest	0.00	2110.23	105.39	0.81	0.45	0.00	2216.88
	Grassland	98.82	21.60	21,780.00	17.55	14.76	2.25	21,934.98
	Settlement	0.00	0.00	0.00	12.60	0.00	0.00	12.60
	Bare Land	35.91	0.27	619.47	1.08	9476.19	0.00	10,132.92
	Others	0.00	0.00	0.00	0.00	0.00	36.27	36.27
	Total Area	5277.51	2132.19	22,517.37	35.01	9491.40	38.52	39,492.00
		2010						
	Land Use Types	**Cropland**	**Forest**	**Grassland**	**Settlement**	**Bare Land**	**Others**	**Total Area**
2005	Cropland	5241.51	0.00	32.85	3.15	0.00	0.00	5277.51
	Forest	0.00	2058.39	71.73	1.80	0.27	0.00	2132.19
	Grassland	21.24	0.99	22,424.58	16.11	52.02	2.43	22,517.37
	Settlement	0.00	0.00	0.00	35.01	0.00	0.00	35.01
	Bare Land	2.16	0.00	106.83	0.36	9382.05	0.00	9491.40
	Others	0.00	0.00	0.00	0.00	0.00	38.52	38.52
	Total Area	5264.91	2059.38	22,635.99	56.43	9434.34	40.95	39,492.00
		2015						
	Land Use Types	**Cropland**	**Forest**	**Grassland**	**Settlement**	**Bare Land**	**Others**	**Total Area**
2010	Cropland	5167.08	0.09	90.27	7.38	0.09	0.00	5264.91
	Forest	0.00	1934.82	123.66	0.90	0.00	0.00	2059.38
	Grassland	0.09	1.80	22,599.90	16.92	16.20	1.08	22,635.99
	Settlement	0.00	0.00	0.00	56.43	0.00	0.00	56.43
	Bare Land	0.00	0.00	369.27	0.00	9065.07	0.00	9434.34
	Others	0.00	0.00	0.00	0.00	0.00	40.95	40.95
	Total Area	5167.17	1936.71	23,183.10	81.63	9081.36	42.03	39,492.00
		2018						
	Land Use Types	**Cropland**	**Forest**	**Grassland**	**Settlement**	**Bare Land**	**Others**	**Total Area**
2015	Cropland	5104.53	0.27	57.87	4.41	0.09	0.00	5167.17

Forest	0.00	1903.50	32.85	0.36	0.00	0.00	1936.71
Grassland	21.87	4.41	23,104.08	16.83	35.73	0.18	23,183.10
Settlement	0.00	0.00	0.00	81.63	0.00	0.00	81.63
Bare Land	4.59	0.00	31.50	0.81	9044.46	0.00	9081.36
Others	0.00	0.00	0.00	0.00	0.00	42.03	42.03
Total Area	5130.99	1908.18	23,226.30	104.04	9080.28	42.21	39,492.00

Notes: Yellow filled numbers denote the parts of land use that did not change during any two periods.

Appendix D

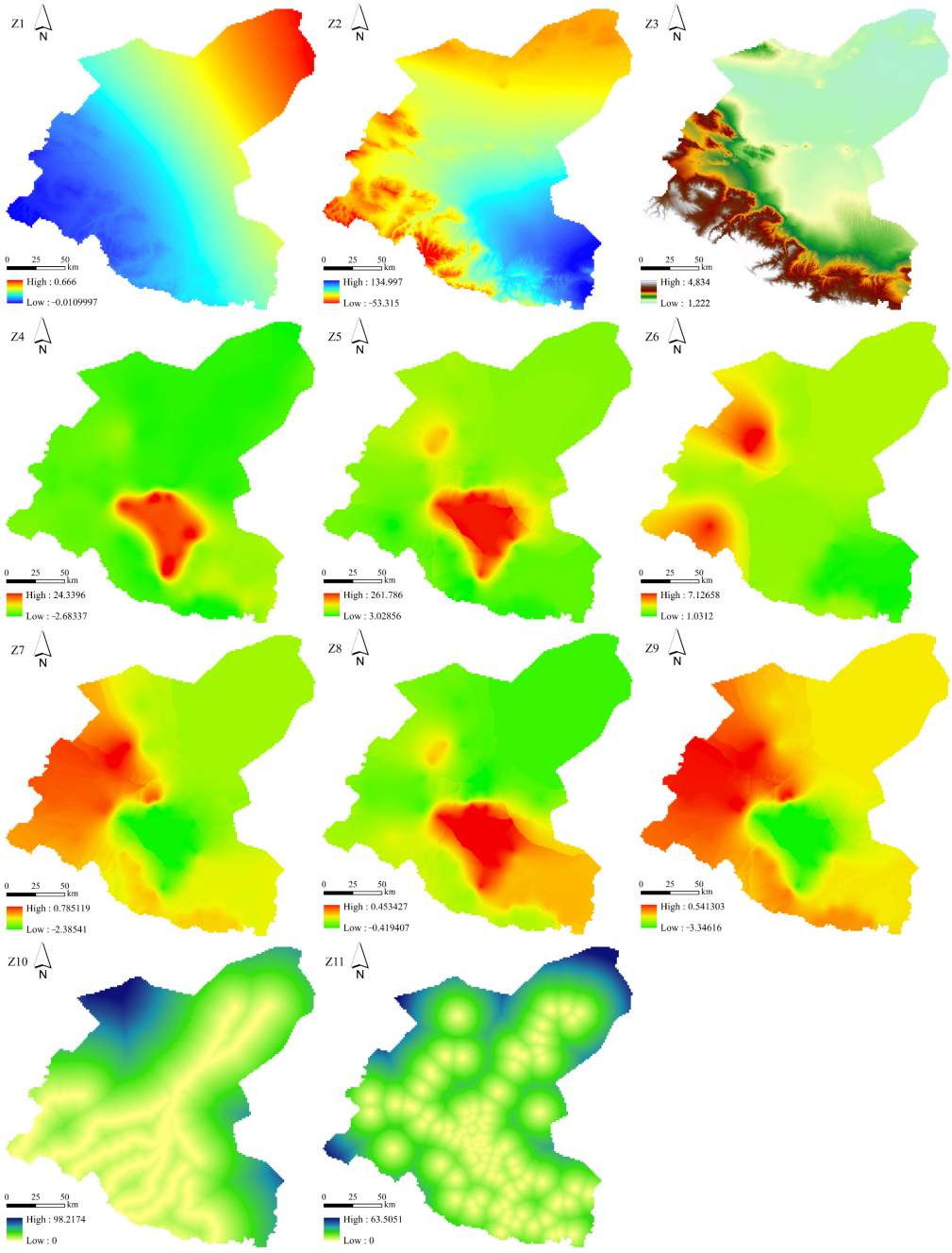

Figure A2. Spatial distributions of the factors for the driving analysis of LULC changes from 2000 to 2018 in the SRB. Notes: The factor codes are as follows: Z1, temperature; Z2, precipitation; Z3, altitude; Z4, population density; Z5, GDP; Z6, GDP per capita; Z7, total water consumption; Z8,

surface water supply; Z9, groundwater supply; Z10, distance to the rivers; and Z11, distance to urban and township centers. The meaning of each factor is detailed in Table 2 in the manuscript.

Appendix E

Table A3. Factor detector results of different main LULC changes in the SRB.

LULC Change Type	Z1	Z2	Z3	Z4	Z5	Z6	Z7	Z8	Z9	Z10	Z11
CTG	0.0181	0.0039	0.0090	0.0152	0.0054	0.0019	0.0162	0.0099	0.0136	0.0110	0.0071
CTS	0.0092	0.0055	0.0058	0.0108	0.0104	0.0018	0.0125	0.0105	0.0112	0.0025	0.0109
FTG	0.0307	0.0034	0.0311	0.0196	0.0019	0.0075	0.0201	0.0161	0.0183	0.0102	0.0035
GTB	0.0122	0.0036	0.0088	0.0056	0.0042	0.0029	0.0070	0.0068	0.0047	0.0014	0.0037
GTC	0.0032	0.0146	0.0105	0.0030	0.0047	0.0035	0.0048	0.0030	0.0065	0.0033	0.0077
GTS	0.0123	0.0071	0.0090	0.0064	0.0143	0.0136	0.0200	0.0078	0.0105	0.0028	0.0132
BTC	0.0033	0.0083	0.0037	0.0001	0.0010	0.0006	0.0006	0.0004	0.0006	0.0012	0.0033
BTG	0.0119	0.0080	0.0349	0.0060	0.0203	0.0073	0.0049	0.0139	0.0033	0.0445	0.0219
OTS	0.0041	0.0016	0.0055	0.0009	0.0030	0.0012	0.0075	0.0052	0.0039	0.0032	0.0031

Notes: The factor codes are as follows: CTG, cropland→grassland; CTS, cropland→settlement; FTG, forest→grassland; GTB, grassland→bare land; GTC, grassland→cropland; GTS, grassland→settlement; BTC, bare land→cropland; BTG, bare land→grassland; OTS, other land use conversion types; Z1, temperature; Z2, precipitation; Z3, altitude; Z4, population density; Z5, GDP; Z6, GDP per capita; Z7, total water consumption; Z8, surface water supply; Z9, groundwater supply; Z10, distance to the rivers; and Z11, distance to urban and township centers. The meaning of each factor is detailed in Table 2 in manuscript. Numbers marked in yellow indicate that the *p* value was greater than 0.05 and failed to pass the significance test.

Appendix F

Table A4. Discretization methods and levels of potential driving factors of the main LULC changes in the SRB.

Factor	Level_1	Level_2	Level_3	Level_4	Level_5	Level_6	Level_7	Level_8	Method
Z1 (°C)	[−0.01, 0.09]	(0.09, 0.16]	(0.16, 0.23]	(0.23, 0.29]	(0.29, 0.36]	(0.36, 0.45]	(0.45, 0.55]	(0.55, 0.67]	Natural Breaks
Z2 (mm)	[−53.32, −9.92]	(−9.92, 9.21]	(9.21, 23.92]	(23.92, 39.37]	(39.37, 57.76]	(57.76, 79.09]	(79.09, 101.90]	(101.90, 135.00]	Natural Breaks
Z3 (m)	[1228, 1350]	(1350, 1439]	(1439, 1579]	(1579, 1940]	(1940, 2633]	(2633, 4795]			Quantile
Z4 (persons/km^2)	[−2.68, −0.78]	(−0.78, 2.38]	(2.38, 7.77]	(7.77, 14.84]	(14.84, 24.34]				Natural Breaks
Z5 (10^4 CNY/ km^2)	[3.03, 52.56]	(52.56, 83.89]	(83.89, 128.36]	(128.36, 198.11]	(198.11, 261.79]				Natural Breaks
Z6 (10^4 CNY/ km^2)	[1.03, 2.01]	(2.01, 3.22]	(3.22, 4.27]	(4.27, 5.46]	(5.46, 7.13]				Natural Breaks
Z7 (10^8 m^3/ km^2)	[−2.39, −2.00]	(−2.00, −1.61]	(−1.61, −1.20]	(−1.20, −0.80]	(−0.80, −0.42]	(−0.42, 0.01]	(0.01, 0.327]	(0.33, 0.79]	Natural Breaks
Z8 (10^8 m^3/ km^2)	[−0.42, −0.28]	(−0.28, −0.15]	(−0.15, 0.01]	(0.01, 0.17]	(0.17, 0.31]	(0.31, 0.45]			Natural Breaks
Z9 (10^8 m^3/ km^2)	[−3.35, −2.72]	(−2.72, −2.04]	(−2.04, −1.48]	(−1.48, −0.89]	(−0.89, −0.16]	(−0.16, 0.54]			Natural Breaks
Z10 (km)	[0, 6.38]	(6.38, 14.15]	(14.15, 23.26]	(23.26, 32.90]	(32.90, 43.72]	(43.72, 56.96]	(56.96, 73.50]	(73.50, 98.22]	Natural Breaks

Z11 (km)	[0, 5.82]	(5.82, 10.36]	(10.36, 15.21]	(15.21, 20.44]	(20.44, 26.65]	(26.65, 34.35]	(34.35, 44.26]	(44.26, 63.51]	Natural Breaks

Notes: The factor codes are as follows: Z1, temperature; Z2, precipitation; Z3, altitude; Z4, population density; Z5, GDP; Z6, GDP per capita; Z7, total water consumption; Z8, surface water supply; Z9, groundwater supply; Z10, distance to the rivers; and Z11, distance to urban and township centers. The meaning of each factor is detailed in Table 2 in manuscript.

References

1. Li, X.; Cheng, G.; Ge, Y.; Li, H.; Han, F.; Hu, X.; Tian, Y.; Pan, X.; Nian, Y. Hydrological cycle in the Heihe River Basin and its implication for water resource management in endorheic basins. *J. Geophys. Res. Atmos.* **2018**, *123*, 890–914.
2. Yu, Y.; Pi, Y.; Yu, X.; Ta, Z.; Sun, L.; Disse, M.; Zeng, F.; Li, Y.; Chen, X.; Yu, R. Climate change, water resources and sustainable development in the arid and semi-arid lands of Central Asia in the past 30 years. *J. Arid Land* **2019**, *11*, 1–14.
3. Montenegro, S.; Ragab, R. Impact of possible climate and land use changes in the semi arid regions: A case study from North Eastern Brazil. *J. Hydrol.* **2012**, *434*, 55–68.
4. Bie, Q.; Xie, Y. The constraints and driving forces of oasis development in arid region: A case study of the Hexi Corridor in northwest China. *Sci. Rep.* **2020**, *10*, 17708.
5. Ketema, H.; Wei, W.; Legesse, A.; Wolde, Z.; Temesgen, H.; Yimer, F.; Mamo, A. Quantifying smallholder farmers' managed land use/land cover dynamics and its drivers in contrasting agro-ecological zones of the East African Rift. *Global Ecol. Conserv.* **2020**, *21*, e898.
6. Xi, X.; Sokolik, I.N. Quantifying the anthropogenic dust emission from agricultural land use and desiccation of the Aral Sea in Central Asia. *J. Geophys. Res. Atmos.* **2016**, *121*, 12,270–12,281.
7. El-Tantawi, A.M.; Bao, A.; Chang, C.; Liu, Y. Monitoring and predicting land use/cover changes in the Aksu-Tarim River Basin, Xinjiang-China (1990–2030). *Environ. Monit. Assess.* **2019**, *191*, 480.
8. Zhang, L.; Nan, Z.; Xu, Y.; Li, S. Hydrological impacts of land use change and climate variability in the headwater region of the Heihe River Basin, Northwest China. *PLoS ONE* **2016**, *11*, e158394.
9. Kleemann, J.; Baysal, G.; Bulley, H.N.; Fürst, C. Assessing driving forces of land use and land cover change by a mixed-method approach in north-eastern Ghana, West Africa. *J. Environ. Manag.* **2017**, *196*, 411–442.
10. Zhou, J.; Li, Q.; Wang, L.; Lei, L.; Zhu, G. Impact of climate change and land-use on the propagation from meteorological drought to hydrological drought in the eastern Qilian Mountains. *Water* **2019**, *11*, 1602.
11. Wei, W.; Xie, Y.; Shi, P.; Zhou, J.; Li, C. Spatial temporal analysis of land use change in the Shiyang River Basin in arid China, 1986–2015. *Pol. J. Environ. Stud.* **2017**, *26*, 1789–1796.
12. Wei, W.; Li, Z.; Xie, B.; Zhou, J.; Li, C. Spatio-temporal change and driving force of oasis for desert reservoir from 1988 to 2016 in northwestern China. *Pol. J. Environ. Stud.* **2019**, *29*, 871–884.
13. Lu, H.; Nie, Z.; Liu, M.; Feng, B.; Cheng, X.; Wang, J.; Wang, Q.; Cui, H.; Fan, F. Research on land cover changes in Shiyang River Basin in recent 50 years based on RS and GIS. *Geol. Resour.* **2020**, *29*, 165–171, 179.
14. Hailu, A.; Mammo, S.; Kidane, M. Dynamics of land use, land cover change trend and its drivers in Jimma Geneti District, Western Ethiopia. *Land Use Policy* **2020**, *99*, 105011.
15. Jia, Y.; Yan, L.; Fan, Y.; Cao, L. Land use change and landscape pattern of typical semi-arid and arid watershed of western China: A case study on Shiyang River Basin. *Remote Sens. Inf.* **2016**, *31*, 66–73.
16. Zhang, Y.; Wang, T.; Cai, C.; Li, C.; Liu, Y.; Bao, Y.; Guan, W. Landscape pattern and transition under natural and anthropogenic disturbance in an arid region of northwestern China. *Int. J. Appl. Earth Obs. Geoinf.* **2016**, *44*, 1–10.
17. Guan, H.; Zhang, G. Landscape pattern and its driving forces of Shiyang River Basin. *J. Lanzhou Jiaotong Univ.* **2017**, *36*, 93–99.
18. Liu, C.; Zhang, F.; Johnson, V.C.; Duan, P. Spatio-temporal variation of oasis landscape pattern in arid area: Human or natural driving? *Ecol. Indic.* **2021**, *125*, 107495.
19. Wei, W.; Xie, Y.; Wei, X.; Xie, B.; Zhang, Q.; Hao, Y. Land use optimization based on CLUE-S model and ecological security scenario in Shiyang River Basin. *Geomat. Inf. Sci. Wuhan Univ.* **2017**, *46*, 1306–1315.
20. Yaghobi, S.; Faramarzi, M.; Karimi, H.; Sarvarian, J. Simulation of land-use changes in relation to changes of groundwater level in arid rangeland in western Iran. *Int. J. Environ. Sci. Technol.* **2019**, *16*, 1637–1648.
21. Wang, Q.; Guan, Q.; Lin, J.; Luo, H.; Tan, Z.; Ma, Y. Simulating land use/land cover change in an arid region with the coupling models. *Ecol. Indic.* **2021**, *122*, 107231.
22. Su, F.; Shang, H.; Zhang, Z. The change and analysis on the ecological service of Shiyang River basin from 1980 to 2010. *J. Glaciol. Geocryol.* **2017**, *39*, 917–925.
23. Wang, Y.; Zhao, J.; Fu, J.; Wei, W. Effects of the Grain for Green Program on the water ecosystem services in an arid area of China-Using the Shiyang River Basin as an example. *Ecol. Indic.* **2019**, *104*, 659–668.
24. Yang, L.; Sun, Z.; Li, J.; Shi, L.; Kong, H.; Yang, Y.; Li, T. Spatiotemporal patterns and driving forces of land-use and land-cover change in the Mu Us Sandy Land, China from 1980 to 2018. *Arid Land Res. Manag.* **2021**, *36*, 109–124.

25. Maimaitiaili, A.; Aji, X.; Matniyaz, A.; Kondoh, A. Monitoring and analysing land use/cover changes in an arid region based on multi-satellite data: The Kashgar Region, Northwest China. *Land* **2018**, *7*, 6.
26. Zhao, R.; Chen, Y.; Shi, P.; Zhang, L.; Pan, J.; Zhao, H. Land use and land cover change and driving mechanism in the arid inland river basin: A case study of Tarim River, Xinjiang, China. *Environ. Earth Sci.* **2013**, *68*, 591–604.
27. Zewdie, M.; Worku, H.; Bantider, A. Temporal dynamics of the driving factors of urban landscape change of Addis Ababa during the past three decades. *Environ. Manag.* **2018**, *61*, 132–146.
28. Wu, D.; Feng, X.; Wen, Q. The research of evaluation for growth suitability of Carya Cathayensis Sarg. based on PCA and AHP. *Procedia Eng.* **2011**, *15*, 1879–1883.
29. Kurek, K.A.; Heijman, W.; van Ophem, J.; Gędek, S.; Strojny, J. Measuring local competitiveness: Comparing and integrating two methods PCA and AHP. *Qual. Quant.* **2022**, *56*, 1371–1389.
30. Kang, S.; Su, X.; Tong, L.; Shi, P.; Yang, X.; Abe, Y.; Du, T.; Shen, Q.; Zhang, J. The impacts of human activities on the water–land environment of the Shiyang River Basin, an arid region in northwest China. *Hydrol. Sci. J.* **2004**, *49*, 413–427.
31. Zhou, Y.; Li, X.; Liu, Y. Land use change and driving factors in rural China during the period 1995–2015. *Land Use Policy* **2020**, *99*, 105048.
32. Huang, H.; Zhou, Y.; Qian, M.; Zeng, Z. Land use transition and driving forces in Chinese Loess Plateau: A case study from Pu County, Shanxi Province. *Land* **2021**, *10*, 67.
33. Wang, J.; Xu, C. Geodetector: Principle and prospective. *Acta Geogr. Sin.* **2017**, *72*, 116–134.
34. Huang, F.; Ochoa, C.G.; Chen, X.; Zhang, D. Modeling oasis dynamics driven by ecological water diversion and implications for oasis restoration in arid endorheic basins. *J. Hydrol.* **2021**, *593*, 125774.
35. Xue, D.; Zhou, J.; Zhao, X.; Liu, C.; Wei, W.; Yang, X.; Li, Q.; Zhao, Y. Impacts of climate change and human activities on runoff change in a typical arid watershed, NW China. *Ecol. Indic.* **2021**, *121*, 107013.
36. Liu, M.; Li, L.; Shi, Z.; Qin, S. Distribution characteristics of runoff in Shiyang River Basin and its responses to climate change-The case study of Xiying River. *Agric. Res. Arid Areas* **2013**, *31*, 193–198.
37. Li, Y.; Ge, J.; Hou, M.; Gao, H.; Liu, J.; Bao, X.; Yin, J.; Gao, J.; Feng, Q.; Liang, T. A study of the spatiotemporal dynamic of land cover types and the driving forces of grassland area change in Gannan Prefecture and Northwest Sichuan based on CCI-LC data. *Acta Prataculturae Sin.* **2020**, *29*, 1–15.
38. Wang, H.; Wen, X.; Wang, Y.; Cai, L.; Peng, D.; Liu, Y. China's land cover fraction change during 2001–2015 based on remote sensed data fusion between MCD12 and CCI-LC. *Remote Sens.* **2021**, *13*, 341.
39. Yang, Y.; Xiao, P.; Feng, X.; Li, H. Accuracy assessment of seven global land cover datasets over China. *ISPRS J. Photogramm. Remote Sens.* **2017**, *125*, 156–173.
40. Sun, W.; Ding, X.; Su, J.; Mu, X.; Zhang, Y.; Gao, P.; Zhao, G. Land use and cover changes on the Loess Plateau: A comparison of six global or national land use and cover datasets. *Land Use Policy* **2022**, *119*, 106165.
41. Hua, T.; Zhao, W.; Liu, Y.; Wang, S.; Yang, S. Spatial consistency assessments for global land-cover datasets: A comparison among GLC2000, CCI LC, MCD12, GLOBCOVER and GLCNMO. *Remote Sens.* **2018**, *10*, 1846.
42. Liu, Q.; Zhang, Y.; Liu, L.; Li, L.; Qi, W. The spatial local accuracy of land cover datasets over the Qiangtang Plateau, High Asia. *J. Geogr. Sci.* **2019**, *29*, 1841–1858.
43. Liu, Z.; Li, L.; Tim, R.M.; van Niel, T.G.; Yang, Q.; Li, R. Introduction of the professional interpolation software for meteorology data: ANUSPLINN. *Meteorol. Mon.* **2008**, *34*, 92–100.
44. Qian, Y.; Lv, H.; Zhang, Y. Application and assessment of spatial interpolation method on daily meteorological elements based on ANUSPLIN software. *J. Meteorol. Environ.* **2010**, *26*, 7–15.
45. Ma, H.; Zhang, L.; Wei, X.; Shi, T.; Chen, T. Spatial and temporal variations of land use and vegetation cover in Southwest China from 2000 to 2015. Chin. *J. Appl. Ecol.* **2021**, *32*, 618–628.
46. Zhu, L.; Meng, J.; Zhu, L. Applying Geodetector to disentangle the contributions of natural and anthropogenic factors to NDVI variations in the middle reaches of the Heihe River Basin. *Ecol. Indic.* **2020**, *117*, 106545.
47. Wei, W.; Guo, Z.; Xie, B.; Zhou, J.; Li, C. Spatiotemporal evolution of environment based on integrated remote sensing indexes in arid inland river basin in Northwest China. *Environ. Sci. Pollut. Res.* **2019**, *26*, 13062–13084.
48. Khoshnava, S.M.; Rostami, R.; Zin, R.M.; Kamyab, H.; Abd Majid, M.Z.; Yousefpour, A.; Mardani, A. Green efforts to link the economy and infrastructure strategies in the context of sustainable development. *Energy* **2020**, *193*, 1297–1309.
49. Shi, P.; Wang, Z.; Liu, C. Spatial evolution process, pattern and mechanism of land cover change in Shiyang River Basin. *Acta Ecol. Sin.* **2014**, *34*, 4361–4371.
50. Guan, Q.; Yang, L.; Pan, N.; Lin, J.; Xu, C.; Wang, F.; Liu, Z. Greening and browning of the Hexi Corridor in northwest China: Spatial patterns and responses to climatic variability and anthropogenic drivers. *Remote Sens.* **2018**, *10*, 1270.
51. Li, L.; Wang, D.; Han, T. Spatial-temporal dynamics of vegetation coverage and responding to climate change in Shiyang River Basin during 2000–2015. *J. Desert Res.* **2018**, *38*, 1108–1118.
52. Eamus, D.; Froend, R.; Loomes, R.; Hose, G.; Murray, B. A functional methodology for determining the groundwater regime needed to maintain the health of groundwater-dependent vegetation. *Aust. J. Bot.* **2006**, *54*, 97–114.
53. Glazer, A.N.; Likens, G.E. The water table: The shifting foundation of life on land. *Ambio* **2012**, *41*, 657–669.

54. Huang, F.; Chunyu, X.; Zhang, D.; Chen, X.; Ochoa, C.G. A framework to assess the impact of ecological water conveyance on groundwater-dependent terrestrial ecosystems in arid inland river basins. *Sci. Total Environ.* **2020**, *709*, 136155.
55. Ren, L.; Ran, Y.; Ren, L.; Tan, M. Temporal-spatial characteristics of vegetation change in Shiyang River basin from 2001 to 2018 and its implication for integrated watershed management. *J. Glaciol. Geocryol.* **2019**, *41*, 1244–1253.
56. Zhang, S.; An, F.; Guo, Y. Research on land use change of Shiyang River Basin based on TM image. *Environ. Prot. Xinjiang* **2012**, *34*, 40–46.
57. Chen, Y.; Li, Z.; Fan, Y.; Wang, H.; Fang, G. Research progress on the impact of climate change on water resources in the arid region of Northwest China. *Acta Geogr. Sin.* **2014**, *69*, 1295–1304.
58. Zhang, Y.; Yang, Z.; Wang, L.; Kang, Y. Response of vegetation coverage to climatic factors in the middle reaches of the Shiyang River in growing season. *Arid Zone Res.* **2018**, *35*, 662–668.
59. Li, K.; Feng, M.; Biswas, A.; Su, H.; Niu, Y.; Cao, J. Driving factors and future prediction of land use and cover change based on satellite remote sensing data by the LCM model: A case study from Gansu province, China. *Sensors* **2020**, *20*, 2757.
60. Cao, L.; Nie, Z.; Liu, M.; Lu, H.; Wang, L. Changes in natural vegetation growth and groundwater depth and their relationship in the Minqin oasis in the Shiyang River Basin. *Hydrogeol. Eng. Geol.* **2020**, *47*, 25–33.
61. Jiang, Y.; Yang, J.; Zhao, F.; Hong, K.; Liu, X.; Hao, Y. Effect evaluation on the comprehensive management for Shiyang River Basin from the perspective of temporal and spatial changes of vegetation coverage in Minqin Basin. *J. Yunnan Agric. Univ. Nat. Sci.* **2020**, *35*, 726–735.
62. Wang, J.; Wang, X. Dynamic change characteristics of vegetation coverage in the northern basin of Shiyang River from 2000 to 2016. *Geospat. Inf.* **2019**, *17*, 46–49, 11.
63. Zhang, Y.; Chen, J.; Han, Y.; Qian, M.; Guo, X.; Chen, R.; Xu, D.; Chen, Y. The contribution of Fintech to sustainable development in the digital age: Ant forest and land restoration in China. *Land Use Policy* **2021**, *103*, 105306.
64. Kuang, W. 70 years of urban expansion across China: Trajectory, pattern, and national policies. *Sci. Bull.* **2020**, *65*, 1970–1974.
65. Ding, W.; Liu, Y.; Tian, X.; Zhang, H. A research on innovative management mechanism of Qilian Mountain National Nature Reserve. *Environ. Prot.* **2018**, *46*, 41–46.
66. Xue, X.; Liao, J.; Hsing, Y.; Huang, C.; Liu, F. Policies, land Use, and water resource management in an arid oasis ecosystem. *Environ. Manag.* **2015**, *55*, 1036–1051.
67. Yang, H.; Li, Y.; Feng, Q.; Chen, L.; Zhao, Y. Environmental policy evaluation from the perspective of farmers' perception in arid oasis ecosystem: Experiences of Minqin, Northwest China. *Glob. NEST J.* **2017**, *19*, 289–299.
68. Sun, Q.; Zhang, P.; Sun, D. Analysis of policy effects on land deterioration control in Minqin County, Gansu, Northwest China. *J. Soil Sci.* **2018**, *49*, 1060–1065.
69. Yue, W.; Liu, X.; Wang, T.; Chen, X. Impacts of water saving on groundwater balance in a large-scale arid irrigation district, Northwest China. *Irrig. Sci.* **2016**, *34*, 297–312.
70. Shi, L.; Zhang, R.; Dong, P.; Shi, P.; Cheng, Z. Research on measures for sustainable and efficient utilization of water resources in Minqin County in arid area with water shortage. *Water Resour. Prot.* **2017**, *33*, 20–25.
71. Jiang, G.; Wang, Z. Scale effects of ecological safety of water-saving irrigation: A case study in the arid inland river basin of Northwest China. *Water* **2019**, *11*, 1886.
72. Cao, L.; Nie, Z.; Liu, M.; Wang, L.; Wang, J.; Wang, Q. The ecological relationship of groundwater–soil–vegetation in the oasis–desert transition zone of the Shiyang River Basin. *Water* **2021**, *13*, 1642.
73. Lei, B.; Liu, Y.; Du, L.; Wang, L.; Peng, Z. Primary research on integrated evaluation of environment impacts by water-saving improvement in irrigation districts. *J. Irrig. Drain* **2011**, *30*, 100–103.
74. Li, W.; Yang, L. China's 13th and 14th Five-Year Plans: Review and advice. *China Econ.* **2020**, *15*, 2–36.